Nuclear Physics B140 (1978) 301–313

RENORMALIZATION OF THE POMERON INTERCEPT IN REGGEON FIELD THEORY ON A TRANSVERSE LATTICE

L. MASPERI *
International Centre for Theoretical Physics, Trieste, Italy

V. ROBERTO
Istituto di Fisica Teorica dell'Università di Trieste, Italy

A. UNGKITCHANUKIT **
International Centre for Theoretical Physics, Trieste, Italy

Received 5 September 1977
(Revised 12 April 1978)

Using the block spin procedure, the negative renormalization of the pomeron intercept near the critical point is estimated to be 0.03 ~ 0.05, in agreement with previous evaluations based on the one-loop approximation of the renormalization group functions.

1. Introduction

Reggeon field theory [1] (RFT) with imaginary triple coupling predicts a negative renormalization of the pomeron intercept. The bare pomeron intercept α_0 which is the object relevant for phenomenology up to ISR rapidities is brought down to its renormalized value α_R at higher rapidities through the pomeron interactions. Theoretically [2], for α_0 below a critical α_0^c (i.e. α_0 subcritical) the system is in a disordered phase and $\alpha_R < 1$; as α_0 increases to α_0^c, α_R reaches unity and remains at this value beyond the critical point when the system enters its ordered phase (i.e. α_0 supercritical). The numerical determination of the intercept renormalization $\alpha_0 - \alpha_R$ is clearly important in clarifying whether the subcritical, critical or supercritical RFT is the relevant theory when compared to experimental data.

Previous non-perturbative calculations of α_0^c were performed using RFT with a momentum transfer cut-off [3] or a rapidity threshold [4]. Both, however, had a possible weak point in their reliance on the one-loop approximation for the evalua-

* Present address: Physics Department, University of California at Santa Barbara, USA. On leave of absence from Centro Atómico Bariloche, Bariloche, Argentina.
** Present address: Theory Division, TIFR, Bombay, India.

tion of the renormalization group functions. As an alternative, the use of RFT on a transverse lattice [2,5,6] can, at least in principle, account for all powers of the triple-pomeron coupling provided the solution of the single-site Hamiltonian is known. This Hamiltonian contains a potential [7] which can be in one of two configurations, depending on the values of the parameters of the theory: the intersite distance b (which can be related to the momentum transfer cut-off), the bare pomeron intercept α_0, slope α_0' and triple coupling r_0. Recent works [2,5] on the analogue spin model of RFT have investigated the theory corresponding to the two-well configuration of the potential (ground and first excited energy levels much lower than the rest) and have achieved much in elucidating the nature of the phase transition which does not depend on the actual values of the parameters. However, in these papers the renormalization of the pomeron intercept and α_0^c, which are non-universal quantities dependent on the "microscopic details" of the theory, have not been evaluated.

In the present work we show that the one-well potential configuration of the single-site Hamiltonian (gap between second and first excited levels not much larger than gap between the latter and the ground state) is the appropriate starting point for realistic values of the parameters. Keeping only the two lower levels and following the block spin procedure we obtain a phase transition with critical exponents in agreement with those of ref. [5], which is to be expected because of their universal character. In addition, the intercept renormalization near the critical point is now within reach and is computed giving numerical results consistent with those obtained from the one-loop approximation of the renormalization group functions [3,4].

The gain in the high accuracy with which we can evaluate the influence of r_0 in the single-site energy levels was obtained at a cost in the abrupt cut-off corresponding to the lattice spacing. Furthermore, in the block spin realization of the renormalization group transformations, we were forced to retain only two states of the Hamiltonian for the starting point of each interaction to avoid great calculation complexities. Regarding the approximation due to the crude cutoff, it will be seen that the lowest-order correction to the pomeron propagator will turn out to be numerically similar to that obtained from more reasonable exponential cut-offs [3,4]. For the spin approximation, we shall show that the inclusion of the second excited single-site level introduces only small variations in the energy of the first excited two-site cell state. The error caused by truncating the spectrum in the subsequent steps of the renormalization group technique is expected not to alter the correct order of magnitude of $\alpha_0^c - 1$. This is suggested by the comparison of the block-spin calculation for the one-dimensional Ising model in an external field [8] with the exact result [9] and also by confronting the critical temperature of spin RFT obtained with the block spin method [5] and with the high-temperature expansion [10].

Sect. 2 outlines the single-site limit of the Hamiltonian form of RFT on a transverse lattice. Sect. 3 follows with an account of the inclusion of the intersite interactions and the block spin renormalization group procedure. The results are pre-

sented in sect. 4 and finally in sect. 5 the influence of the truncation of the single-site spectrum and other approximations are assessed and discussed.

2. Single-site solutions of the Hamiltonian

The Hamiltonian for RFT with triple-pomeron coupling in the two-dimensional impact parameter lattice, with spacing b, is given by [2,5,6]

$$H = \sum_j \left\{ \Delta_0 \bar{\psi}_j \psi_j + i \frac{r_0}{2b} \bar{\psi}_j (\psi_j + \bar{\psi}_j) \psi_j \right.$$

$$\left. + \frac{\alpha_0'}{b^2} \sum_{\hat{i}} (\bar{\psi}_{j+\hat{i}} - \bar{\psi}_j)(\psi_{j+\hat{i}} - \psi_j) \right\} , \tag{1}$$

where $\Delta_0 = 1 - \alpha_0$ and $\bar{\psi}_j$ and ψ_j are the pomeron fields at the site denoted by the two-dimensional lattice vector j; $\hat{i}$ is a two-dimensional unit vector which connects each site j with its two nearest neighbours along the positive directions. In terms of the representations [7]

$$\psi_j = i \frac{\partial}{\partial(x_j^2)} , \qquad \bar{\psi}_j = -i x_j^2 , \tag{2}$$

the Hamiltonian, eq. (1), can be written

$$H = \sum_j H_j - \sum_{j\hat{i}} H_{j\hat{i}} , \tag{3}$$

where the single-site and intersite terms are

$$H_j = \Delta_0' x_j^2 \frac{\partial}{\partial(x_j^2)} + \frac{r_0}{2b} \left(x_j^4 \frac{\partial}{\partial(x_j^2)} - x_j^2 \frac{\partial^2}{\partial(x_j^2)^2} \right) ,$$

$$H_{j\hat{i}} = \frac{\alpha_0'}{b^2} \left[x_{j+\hat{i}}^2 \frac{\partial}{\partial(x_j^2)} + x_j^2 \frac{\partial}{\partial x_{j+\hat{i}}^2} \right] ,$$

respectively, with

$$\Delta_0' = \Delta_0 + 4\tilde{\alpha}_0' , \qquad \tilde{\alpha}_0' = \alpha_0'/b^2 .$$

Through a non-unitary similarity transformation [7]

$$\tilde{H}_j = F^{-1} H_j F , \tag{4}$$

with

$$F = x_j^{1/2} \exp\left\{ \tfrac{1}{4} x_j^4 + \frac{\Delta_0'}{r_0/b} x_j^2 \right\} ,$$

the single-site problem reduces to a Schrödinger equation with a potential

$$v(x^2) = x^2\left(x^2 + \frac{2\Delta_0'}{r_0/b}\right)^2 - 2x^2 + \frac{3}{4}\frac{1}{x^2}\,, \tag{5}$$

whose lowest eigenvalue corresponds to the first excited level of H_f since the ground state of the latter is just the vacuum [11].

A study of the potential, eq. (5), reveals that it can assume one of two configurations depending on the ratio of $-\Delta_0'$ to r_0/b. For $-\Delta_0' > 1.65\, r_0/b$ (Δ_0' negative) the potential adopts a two-well structure, its lower eigenvalue lies near the vacuum (zero energy) and in this case the single-site solutions build, approximately, the matrix representations of $\bar{\psi}_j$ and ψ_j used in refs. [2,5,6]. However, with values of the parameters extracted from present data ($\alpha_0' = 0.25\ \mathrm{GeV}^{-2}$, $r_0 = 0.5\ \mathrm{GeV}^{-1}$ and b obtained from the momentum transfer cut-off $-t \approx \pi^2/b^2 \approx 1\ \mathrm{GeV}^2$) the above inequality is not satisfied unless $\alpha_0 \gtrsim 1.5$, which is much higher than the expected α_0^c; therefore, near the critical point the potential takes the one-well configuration and the first excited level of H_f is much above the vacuum.

Since the general properties of the phase transition are universal and are not affected by the numerical values of the parameters, the choice of arbitrarily small r_0 and α_0' has allowed the calculation of the critical exponents starting from the two-well potential [5]. On the other hand, the intercept renormalization and α_0^c do depend on the actual values of the parameters and their computation is inaccessible from the two-well configuration. To explore the values of α_0 in the vicinity of the critical point we must start therefore from the one-well configuration, whose eigenvalues and eigenvectors, unfortunately, cannot be determined analytically.

The basis which diagonalizes the single-site Hamiltonian in the limit $\Delta_0' \gg r_0/b$ (Δ_0' positive) is [7]

$$|0\rangle = 1\,, \qquad \langle 0| = \delta(x)\,,$$

$$|n\rangle = -R^{n-1}\frac{x^2}{n}\,L_{n-1}^1(x^2/R)\,, \qquad n \geqslant 1\,,$$

$$\langle n| = R^{-n}\,\mathrm{e}^{-x^2/R}\left[\delta(x) - \frac{x}{R}\,L_{n-1}^1(x^2/R)\right], \qquad n \geqslant 1\,, \tag{6}$$

where $R = r_0/2b\Delta_0'$, L_p^1 are the generalized Laguerre polynomials [12] and the left and right state vectors are different due to the non-hermiticity of H_f. In this basis it is straightforward to obtain the following matrix representations, valid for any value of the parameters:

$$\begin{aligned}\langle m|H_f|n\rangle = R^{n-m}\Delta_0' \{&n[1 + R^2(3n-1)]\,\delta_{m,n} \\ &-(n-1)(3n-2)\,R^2\delta_{m,n-1} - n(n+1)\,R^2\delta_{m,n+1} \\ &+(n-1)(n-2)\,R^2\delta_{m,n-2}\}\end{aligned} \tag{7}$$

for both $m,n > 0$, and equals zero otherwise;

$$\langle m|x_j^2|n\rangle = -(n+1)\,\delta_{m,n+1} + 2nR\delta_{m,n} - (n-1)\,R^2\delta_{m,n-1}\,, \tag{8}$$

$$\left\langle m\left|\frac{\partial}{\partial(x_j^2)}\right|n\right\rangle = -R^{n-m-1} \tag{9}$$

for $n > m$, and equal zero otherwise.

Since we are primarily interested in the first excited levels because of their relevance at high rapidities, we choose to diagonalize the matrix, eq. (7), retaining only the first N vectors of the basis eq. (6). It is important to note that for a given N, corrections of order up to $R^{2(N-1)}$ are included in this way. Consequently the present method will be reliable as long as $R < 1$, so that for reasonable values of $b < 4$ GeV^{-1} (and realistic α_0' and r_0) the region of negative Δ_0 satisfying $\Delta_0 > (0.25 - 1/b)/b$ can be studied. It is clear that for small value of b one may hope to reach the critical point whereas for b near 4 this region may not be attained because the basis, eq. (6), is not a good starting point. This will prove to be the case, as will be discussed in sect. 4.

3. Intersite interactions and block spin renormalization group procedure

Returning to the total Hamiltonian, eq. (3), to include the intersite interactions but keeping only the two lowest states at each site we arrive at an analogue quantum spin model (with nearest-neighbour interactions) for RFT. This approximation is quite accurate only in the very supercritical region where the second excited state is much higher than the first. In the case we wish to analyze (subcritical and slightly supercritical regions) the second energy gap is not much bigger than the first. However, we keep also here only two levels since the systematic inclusion of the next one presents very hard computational difficulties. Moreover, we will show in sect. 5 that the second excited level of the single-site Hamiltonian produces only a slight shift in the first excited level of the two-site cell, indicating that the spin approximation is fairly good also around the critical point.

Let the $N \times N$ matrix which diagonalizes the single-site Hamiltonian H_j be denoted by T; it will be of the type

$$T = \begin{bmatrix} 1 & 0 & 0 & \dots & 0 \\ 0 & t_{22} & t_{23} & \dots & t_{2N} \\ 0 & t_{32} & t_{33} & \dots & t_{3N} \\ & & & & \\ \cdot & & & & \\ \cdot & & & & \\ \cdot & & & & \\ 0 & t_{N2} & t_{N3} & \dots & t_{NN} \end{bmatrix}. \tag{10}$$

for both $m,n > 0$, and equals zero otherwise;

$$\langle m|x_j^2|n\rangle = -(n+1)\,\delta_{m,n+1} + 2nR\delta_{m,n} - (n-1)\,R^2\delta_{m,n-1}\,, \tag{8}$$

$$\left\langle m\left|\frac{\partial}{\partial(x_j^2)}\right|n\right\rangle = -R^{n-m-1} \tag{9}$$

for $n > m$, and equal zero otherwise.

Since we are primarily interested in the first excited levels because of their relevance at high rapidities, we choose to diagonalize the matrix, eq. (7), retaining only the first N vectors of the basis eq. (6). It is important to note that for a given N, corrections of order up to $R^{2(N-1)}$ are included in this way. Consequently the present method will be reliable as long as $R < 1$, so that for reasonable values of $b < 4$ GeV^{-1} (and realistic α_0' and r_0) the region of negative Δ_0 satisfying $\Delta_0 > (0.25 - 1/b)/b$ can be studied. It is clear that for small value of b one may hope to reach the critical point whereas for b near 4 this region may not be attained because the basis, eq. (6), is not a good starting point. This will prove to be the case, as will be discussed in sect. 4.

3. Intersite interactions and block spin renormalization group procedure

Returning to the total Hamiltonian, eq. (3), to include the intersite interactions but keeping only the two lowest states at each site we arrive at an analogue quantum spin model (with nearest-neighbour interactions) for RFT. This approximation is quite accurate only in the very supercritical region where the second excited state is much higher than the first. In the case we wish to analyze (subcritical and slightly supercritical regions) the second energy gap is not much bigger than the first. However, we keep also here only two levels since the systematic inclusion of the next one presents very hard computational difficulties. Moreover, we will show in sect. 5 that the second excited level of the single-site Hamiltonian produces only a slight shift in the first excited level of the two-site cell, indicating that the spin approximation is fairly good also around the critical point.

Let the $N \times N$ matrix which diagonalizes the single-site Hamiltonian H_j be denoted by T; it will be of the type

$$T = \begin{bmatrix} 1 & 0 & 0 & \dots & 0 \\ 0 & t_{22} & t_{23} & \dots & t_{2N} \\ 0 & t_{32} & t_{33} & \dots & t_{3N} \\ & & & & \\ \cdot & & & & \\ \cdot & & & & \\ \cdot & & & & \\ 0 & t_{N2} & t_{N3} & \dots & t_{NN} \end{bmatrix}. \tag{10}$$

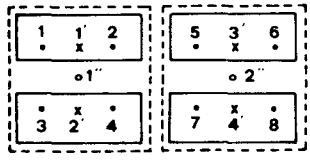

Fig. 1. Two-dimensional lattice with two-site cells. $\overset{n}{\cdot}$ denotes single site, $\overset{n'}{\times}$ single cell and $\overset{n''}{\circ}$ single second step cell.

For the total Hamiltonian the corresponding similarity transformation must then be applied to x^2 and $\partial/\partial x^2$. Since we are interested in the two lowest levels of the Hamiltonian we retain only the top left 2×2 submatrices which are of the forms

$$T^{-1}x^2T \simeq \mu_1 \begin{pmatrix} 0 & 0 \\ 1 & i\tau_1 \end{pmatrix}, \qquad T^{-1}\frac{\partial}{\partial(x^2)}T \simeq \mu_2 \begin{pmatrix} 0 & 1 \\ 0 & i\tau_2 \end{pmatrix}. \tag{11}$$

The matrices T and T^{-1} can be evaluated in terms of the diagonal elements t_{22}, $t_{33}, \ldots t_{NN}$ which are arbitrary. With the condition $\tau_1 = \tau_2 = \tau$, useful for the next steps, the value of t_{22} is fixed, whereas the others may be still arbitrarily chosen.

Defining

$$\rho_{\mathrm{I}} = (\tilde{\alpha}_0'\mu_1\mu_2)^{1/2}, \quad \rho_{\mathrm{II}} = \rho_{\mathrm{I}}\tau, \tag{12}$$

the Hamiltonian of an isolated two-site cell containing sites 1 and 2 may be written (see fig. 1)

$$H_1' = \epsilon(c_1 + c_2) - [(\rho_{\mathrm{I}}\sigma_1^+ + i\rho_{\mathrm{II}}c_1)(\rho_{\mathrm{I}}\sigma_2^- + i\rho_{\mathrm{II}}c_2) + (1 \leftrightarrow 2)], \tag{13}$$

where ϵ is the energy gap between the two lowest single-site levels and

$$c = \begin{pmatrix} 0 & 0 \\ 0 & 1 \end{pmatrix}, \quad \sigma^+ = \begin{pmatrix} 0 & 1 \\ 0 & 0 \end{pmatrix}, \quad \sigma^- = \begin{pmatrix} 0 & 0 \\ 1 & 0 \end{pmatrix}, \tag{14}$$

with the primed index acting as a cell label. In eq. (13) we have obtained an effective quantum spin analogue of RFT which is identical to that of ref. [5] apart from the important differences in the relations of $\epsilon, \rho_{\mathrm{I}}, \rho_{\mathrm{II}}$ with the "microscopic" parameters r_0, α_0', b.

The block spin construction and iterations proceed therefore exactly as in ref. [5] (see fig. 1), keeping only the two lowest levels of each cell for the next iteration and demanding the intercell Hamiltonian to be of the same form as the intersite one. We recall that the recursion relations between the parameters are

$$\epsilon' = \tfrac{1}{2}\{3\epsilon + 2\rho_{\mathrm{II}}^2 - \rho_{\mathrm{I}}^2 - [\epsilon^2 + 2\epsilon(2\rho_{\mathrm{II}}^2 + \rho_{\mathrm{I}}^2) + (2\rho_{\mathrm{II}}^2 - \rho_{\mathrm{I}}^2)^2]^{1/2}\}, \tag{15}$$

$$\rho_{\mathrm{I}}' = 2^{1/4}A\rho_{\mathrm{I}}, \quad \rho_{\mathrm{II}}' = 2^{1/4}[(A^2 - B^2)\rho_{\mathrm{II}} + AB\rho_{\mathrm{I}}], \tag{16}$$

where

$$A = \frac{\rho_I \rho_{II}}{[2\rho_I^2\rho_{II}^2 - (\rho_I^2 + \epsilon' - \epsilon)^2]^{1/2}},$$

$$B = \frac{\rho_I^2 + \epsilon' - \epsilon}{[2\rho_I^2\rho_{II}^2 - (\rho_I^2 + \epsilon' - \epsilon)^2]^{1/2}}. \tag{17}$$

As in ref. [5], the transformations, eqs. (15) and (16). have two types of stable fixed points: one for $\alpha_0 < \alpha_0^c$ (disordered phase) with

$$\epsilon \to \Delta \text{ finite}, \qquad \rho_I, \rho_{II} \to 0,$$

and the other for $\alpha_0 > \alpha_0^c$ (ordered phase) with

$$\epsilon \to 0, \qquad \rho_I = \rho_{II} \neq 0.$$

When a critical point α_0^c is approached from below ($\alpha_0 < \alpha_0^c$), $\Delta \to 0$ with the power behaviour

$$\Delta \sim (\alpha_0^c - \alpha_0)^\nu. \tag{18}$$

In the ordered phase $\rho_I = \rho_{II} = \rho$ is not a fixed value due to the factor $2^{1/4}$ on the right-hand side of eq. (16). Therefore $\sigma = (\frac{1}{2})^{M/4}\rho$, where M is the number of iterations, has a power behaviour as α_0 approaches α_0^c from above

$$\sigma \sim (\alpha_0 - \alpha_0^c)^\beta. \tag{19}$$

σ and Δ are then the order and disorder parameters of the theory giving the critical exponents β and ν which, being independent of the "microscopic details" of the system, are not sensitive to the choice of the potential for the single-site Hamiltonian.

At variance with ref. [5], because of our relations of $\epsilon, \rho_I, \rho_{II}$ with realistic values of r_0, α_0', b, the negative renormalization $\alpha_0 - \alpha_R$ may now be calculated, with $\alpha_R = 1 - \Delta$ being the renormalized intercept of the pomeron. Starting from the disordered phase, as α_0 increases it sweeps past α_0^c where Δ becomes zero giving us the signal that the critical point is reached.

4. Numerical results

A representative sample of the results are summarized in table 1, where $r_0 = 0.5$ GeV^{-1} and $\alpha_0' = 0.25$ GeV^{-2}. For each numerical run the intersite distance b and the bare intercept α_0 are kept constant. Diagonalizing the single-site Hamiltonian, eq. (7), the first excited level ϵ_{in} is evaluated. Through the procedure sketched in eqs. (10), (11) and (12), ρ_{Iin} and ρ_{IIin} are also calculated. These parameters, which are the input for the renormalization group technique, depend on the finite dimension N of the single-site Hamiltonian, but it turns out that they are already prac-

Table 1
Summary of results

b (GeV^{-1})	α_0	ϵ_{in}	ρ_{Iin}	ρ_{IIin}	Δ	σ	$\alpha_0 - \alpha_R$	α_0^c
	0.7	1.38	0.51	−0.19	0.50	0	0.20	
	0.8	1.29	0.51	−0.21	0.41	0	0.21	
	0.9	1.20	0.52	−0.22	0.31	0	0.21	
	1.0	1.10	0.52	−0.24	0.21	0	0.21	
	1.1	1.01	0.52	−0.27	0.12	0	0.22	
1	1.2	0.92	0.53	−0.29	0.03	0	0.23	1.2315
	1.23	0.89	0.53	−0.29	0	0	0.23	
	1.25	0.87	0.53	−0.30	0	0.008		
	1.29	0.83	0.53	−0.30	0	0.026		
	1.33	0.80	0.53	−0.31	0	0.048		
	1.37	0.76	0.53	−0.30	0	0.072		
	1.41	0.72	0.54	−0.29	0	0.102		
	0.7	0.60	0.26	−0.11	0.37	0	0.07	
2	0.8	0.50	0.26	−0.13	0.28	0	0.08	1.09
	0.9	0.41	0.26	−0.15	0.18	0	0.08	
	1.0	0.33	0.27	−0.17	0.09	0	0.09	
	0.7	0.44	0.17	−0.07	0.34	0	0.04	
3	0.8	0.35	0.17	−0.09	0.25	0	0.05	1.05
	0.9	0.25	0.18	−0.10	0.15	0	0.05	
	0.7	0.38	0.13	−0.04	0.33	0	0.03	
4	0.8	0.29	0.13	−0.06	0.23	0	0.03	1.03
	0.9	0.19	0.13	−0.08	0.13	0	0.03	

b is the intersite distance; α_0 the bare intercept; ϵ_{in} the first excited single-site level; ρ_{Iin} and ρ_{IIin} the intersite couplings; Δ the first excited level for the total lattice and σ its order parameter; $\alpha_0 - \alpha_R$ the intercept renormalization and α_0^c the critical intercept.

tically unchanged in passing from $N = 4$ to $N = 5$ for the region of validity of the method; therefore, the results quoted in table 1 correspond to the case for $N = 5$. The fixed-point parameters Δ and σ which are evaluated after a finite number of iterations, allow us to determine the intercept renormalization $\alpha_0 - \alpha_R$ and the critical bare pomeron intercept α_0^c.

From table 1, the critical exponents are obtained giving $\nu \approx 1.03$ and $\beta \approx 1.10$ in agreement with ref. [5]. The other critical exponents γ and z are not calculated since they depend on an unstable fixed point and their determinations do not seem reliable with the present method as observed in ref. [5]. The critical exponents obviously do not depend on b, as can be explicitly checked from table 1 in the case of ν. The universal character of the critical exponents implies that one can choose arbitrarily small values of r_0 and α_0' (to make the two-well potential scheme valid)

for their determination. Thus it can be clearly understood why we obtain good agreement with ref. [5]. In contrast, the critical intercept α_0^c depends on the "microscopic details" and could not be calculated in ref. [5] because the relevant formulae did not hold for realistic values of the parameters. As a consequence, from the critical temperature obtained there $T_c = 2.87 = \epsilon/\rho^2$, where

$$\epsilon \approx \sqrt{\frac{2}{\pi}}\,\Delta_0^2\,\frac{b}{r_0}\exp\left\{-\frac{2\Delta_0^2 b^2}{r_0^2}\right\}, \qquad \rho^2 = 4\alpha_0'\,\frac{\Delta_0^2}{r_0^2},$$

it can be clearly seen that the extraction of the critical value of Δ_0 is impossible.

The value of α_0^c depends on b and is larger for smaller b. For $b = 1$ the ordered phase is within reach and α_0^c is determined with accuracy, while unfortunately for $b \geqslant 2$ the approximation of working with only a finite number of single-site vectors of the basis in eq. (6) becomes inadequate near the critical point (since the condition $2\,\Delta_0' > r_0/b$ is no longer fulfilled) so that the reported values of α_0^c have been estimated from the amount of renormalization in the subcritical region.

Since a reasonable value for the momentum transfer cut-off is at $-t \approx 1\ \mathrm{GeV}^2$, the corresponding value for b is 3–$4\ \mathrm{GeV}^{-1}$ and the resulting critical intercept is $\alpha_0^c \approx 1.03$–1.05. This result is in agreement with the values obtained through the one-loop approximation of the renormalization group functions [3,4].

5. Discussion of approximations

The main approximation in the present calculation lies in our keeping only two states at each iteration. On the other hand, its principal virtue is in the high accuracy obtainable for the evaluation of the one-site levels using a finite N-dimensional basis provided $R < 1$.

We shall assess the accuracy of the spin model relative to an $O(R^2)$ calculation by comparing the values of the two lowest levels for the one-site Hamiltonian (E_1, E_2) and the next two steps (E_1', E_2'), (E_1'', E_2'') obtained following sect. 3, with the corresponding values resulting from the $O(R^2)$ computation.

The first and second excited levels of the one-site Hamiltonian, eq. (7), keeping only terms up to $O(R^2)$, are

$$E_1(2) = \Delta_0'(1 + 2R^2), \qquad E_2(2) = 2\Delta_0'(1 + 5R^2). \tag{20}$$

Considering now the two-site cell Hamiltonian, eq. (13), in the same approximation

$$H_1'(2) = \begin{pmatrix} 0 & 0 \\ 0 & E_1(2) \end{pmatrix}_1 + \begin{pmatrix} 0 & 0 \\ 0 & E_1(2) \end{pmatrix}_2 - \tilde{\alpha}_0'\left[\begin{pmatrix} 0 & 0 \\ -1 & 2R \end{pmatrix}_1 \begin{pmatrix} 0 & -1 \\ 0 & 0 \end{pmatrix}_2 + (1 \leftrightarrow 2)\right], \tag{21}$$

its lowest excited eigenvalues are

$$E_1'(2) = E_1(2) - \tilde{\alpha}_0' , \qquad E_2'(2) = E_1(2) + \tilde{\alpha}_0' . \tag{22}$$

In the same way, diagonalizing the two-cell Hamiltonian

$$H_1''(2) = \begin{pmatrix} 0 & 0 \\ 0 & E_1'(2) \end{pmatrix}_{1'} + \begin{pmatrix} 0 & 0 \\ 0 & E_1'(2) \end{pmatrix}_{2'}$$

$$-\tilde{\alpha}_0' \left\{ \left[\begin{pmatrix} 0 & 0 \\ -1 & 2R \end{pmatrix}_1 \begin{pmatrix} 0 & -1 \\ 0 & 0 \end{pmatrix}_3 + (1 \leftrightarrow 3) \right] + \left[\begin{matrix} 1 \to 2 \\ 3 \to 4 \end{matrix} \right] \right\} , \tag{23}$$

one obtains

$$E_1''(2) = E_1'(2) - \tilde{\alpha}_0' , \qquad E_2''(2) = E_1'(2) + \tilde{\alpha}_0' . \tag{24}$$

The results of the $O(R^2)$ approximation and those of the block-spin model are tabulated in table 2. It is seen that the block spin calculation gives higher first excited levels after two iterations, signifying that the intercept renormalization is larger than that predicted by the second-order calculation in R. Moreover, the difference is more pronounced for α_0 near the critical point.

We now turn to the weak point of the calculation. In contrast to the very supercritical region where the first excited state is almost degenerate with the vacuum and the second and higher excited states are much higher lying, such is not the state of affairs in our case and the truncation of the one-site spectrum to give the spin

Table 2
Approximations and corrections

$b(\mathrm{GeV}^{-1})$	1				3			
α_0	0.7		1.23		0.7		0.9	
ith excitation level	1st	2nd	1st	2nd	1st	2nd	1st	2nd
E_i	1.38	3.00	0.89	2.10	0.44	0.96	0.25	0.65
E_i	1.13	1.64	0.65	1.17	0.41	0.47	0.22	0.28
E_i''	0.95	1.31	0.47	0.83	0.39	0.43	0.20	0.24
$E_i(2)$	1.39	3.08	0.93	2.33	0.44	0.99	0.28	0.75
$E_i'(2)$	1.14	1.64	0.68	1.18	0.41	0.47	0.25	0.31
$E_i''(2)$	0.89	1.39	0.43	0.93	0.38	0.44	0.19	0.25
$E_i'(3)$	1.14	1.66	0.68	1.22	0.41	0.47	0.25	0.31

(E_1, E_2), (E_1', E_2') and (E_1'', E_2'') are the two lowest excited levels for the single-site, single cell and single second-step cell, respectively. $(E_1(2), E_2(2))$, $(E_1'(2), E_2'(2))$ and $(E_1''(2), E_2''(2))$ are the corresponding levels when only terms up to $O(r_0^2)$ are kept. $(E_1'(3))$ are the two lowest excited levels for the two-site cell up to order $O(r_0^2)$ when three levels are included in the one-site Hamiltonian.

$|t| \sim 1$ GeV^2 of the triple-pomeron coupling, the abrupt cut-off implied by the lattice approximation modifies the theory for $r_0 = 0$ with respect to a simple Regge pole. However, it is easy to verify that this modification is not important as long as $-t << \pi^2/b^2$. Furthermore the $O(r_0^2)$ correction to the pomeron propagator evaluated with the abrupt cut-off

$$\frac{r_0^2}{16\pi\alpha_0'} \ln\left(\frac{\pi^2/b^2 - E/2\alpha_0'}{-E/2\alpha_0'}\right),$$

with $E = 1 - J$, and that obtained from a more realistic exponential cut-off [3]

$$\frac{r_0^2}{16\pi\alpha_0'} e^{-E/\alpha_0'} E_1\left(-\frac{E}{\alpha_0'}\right),$$

where E_1 is the exponential integral function, give similar contributions for $b \approx 4$ GeV^{-1}. Therefore a value of b close to this is a reasonable one to use.

In conclusion, the present paper shows that a phase transition similar to the one studied in ref. [5] occurs in RFT starting from realistic parameters even though the single-site Hamiltonian does not correspond to a two-well potential. In addition, the order of magnitude of $\alpha_0^c - 1$ is evaluated, its precise value being unreliable because of all the approximations involved. From a phenomenological point of view it therefore seems unlikely that the value [13] $\alpha_0^c \approx 1.12$ needed if a secondary vacuum singularity P′ is present may correspond to a critical pomeron. On the contrary [14], if no P′ exists, a critical pomeron with $\alpha_0^c \approx 1.04$ has a chance to reproduce experimental data.

One of us (L.M.) wishes to thank the Theory Division of CERN and the Physics Department of the University of California at Santa Barbara for hospitality during part of this work and OAS and INFN for partial support. We are grateful to D. Amati, G. Calucci, J. Cardy, R. Jengo and M. Le Bellac for extremely valuable comments and to G. Furlan for reading the manuscript. Two of us (L.M. and A.U.) would like to thank Professor Abdus Salam, the International Atomic Energy Agency and UNESCO for hospitality at the International Centre for Theoretical Physics, Trieste.

References

[1] H.D.I. Abarbanel, J.B. Bronzan, R.L. Sugar and A.R. White, Phys. Reports 21 (1975) 119; A.R. White, Lectures at Les Houches, Inst. of Theoretical Physics (1975); M. Moshe, Phys. Reports 37 (1978) 255.
[2] D. Amati, M. Ciafaloni, M. Le Bellac and G. Marchesini, Nucl. Phys. B112 (1976) 107.
[3] W.R. Frazer, H. Hoffman, J.R. Fulco and R.L. Sugar, Phys. Rev. D14 (1976) 2387.
[4] A. García, C.A. García Canal and L. Masperi, Phys. Lett. 66B (1977) 442.
[5] J.L. Cardy, Nucl. Phys. B115 (1976) 141.
[6] R.C. Brower, M.A. Furman and K. Subbarao, Phys. Rev. D15 (1977) 1756.

[7] R. Jengo, Nucl. Phys. B108 (1976) 447.
[8] M. Weinstein, Stanford preprint SLAC-PUB-1854 (1976).
[9] D.J. Scalapino and B. Stoeckly, Phys. Rev. D14 (1976) 3376.
[10] R.C. Brower, M.A. Furman and M. Moshe, CERN preprint TH-2458 (1978).
[11] M. Ciafaloni, M. Le Bellac and G.C. Rossi, Nucl. Phys. 130B (1977) 388.
[12] M. Abramowitz and J. Stegun, Handbook of mathematical functions (Dover Publications, New York, 1965).
[13] A. Capella, J. Kaplan and J. Tran Than Van, Nucl. Phys. B97 (1975) 493; B105 (1976) 333.
[14] A. Della Selva, L. Masperi, V. Roberto and A. Ungkitchanukit, Nucl. Phys. B127 (1977) 413;
L. Masperi, Phys. Lett. 73B (1978) 335.